© 2022 Hefei Institutes of Physical Science, Chinese Academy of Sciences and IOP Publishing Printed in China and the UK

Plasma Sci. Technol. **24** (2022) 085501 (7pp) https://doi.org/10.1088/2058-6272/ac6795

Wideband radar cross-section reduction using plasma-based checkerboard metasurface

Zhiming ZHAO (赵智明), Xiaoping LI (李小平), Guoxiang DONG (董果香)* and Yanming LIU (刘彦明)

School of Aerospace Science and Technology, Xidian University, Xi'an 710126, People's Republic of China

E-mail: gxdong@xidian.edu.cn

Received 15 September 2021, revised 13 April 2022
Accepted for publication 14 April 2022
Published 29 June 2022



Abstract

For stealth technology, in order to overcome the limitations of thin-layer plasma for electromagnetic waves attenuation and further broaden the radar cross-section (RCS) reduction (RCSR) band of the metasurface, the plasma-based checkerboard metasurface composed of plasma and checkerboard metasurface is investigated to achieve better RCSR. We designed a checkerboard metasurface which can achieve abnormal reflection to reduce RCS and whose −10 dB RCSR bandwidth is from 8.1 to 14.5 GHz, the RCSR principle of it lies in the backscattering cancellation, which depends on the phase difference of artificial magnetic conductor (AMC) units. The designed plasma-based checkerboard metasurface is a thin composite structure, including a checkerboard metasurface, a plasma layer, and an air gap which is between them. Full wave simulations confirm that the plasma-based checkerboard metasurface's –10 dB RCS reduction bandwidth and RCS reduction amplitude, are both increased under different polarized waves compared with the only single plasma or the only metasurface. We also introduced the reason and mechanism of the interaction between plasma and the checkerboard metasurface to improve the RCSR effect in detail. As plasma-based checkerboard metasurface does not need the plasma to be too thick for plasma stealth, its application in practical scenarios is easier to implement.

Keywords: abnormal reflection, plasma-based checkerboard metasurface, radar cross section reduction (RCSR), stealth technology

(Some figures may appear in colour only in the online journal)

1. Introduction

As anti-stealth technologies continue to prosper, stealth materials that are featured with wideband and wide-angle characteristics have emerged as the trend for the next generation of stealth equipment.

One new stealth technology is metasurface. Metasurface is a kind of periodic structure array with sub wavelength size which can flexibly and effectively manipulate the phase, amplitude and propagation mode of incident waves [1–3]. Metasurface can be widely applied in fields of stealth radar and with the advantage of small size, light weight and good adaptability to different object geometries [4–9].

In recent years, metasurfaces with low RCS have attracted significant attention worldwide [10–12]. This type of metasurface can reflect normal incident electromagnetic (EM) waves to the other direction, which greatly reduces the RCS of the object covered by the metasurface [13–16]. Checkerboard metasurface is a kind of this metasurface used in stealth technology and can achieve wideband RCSR. It reduces the RCS of target based on the principle of backscattering cancellation between the reflected waves of two different AMC units. In 2013, Galarregui *et al* used two Jerusalem cross structures with different sizes to form a checkerboard structure, achieving a monostatic RCSR of more

* Author to whom any correspondence should be addressed.

than 10 dB at the frequency band ranging from 14.8 to 22.7 GHz [17]. In recent years, the key issue is how to broaden the RCSR bandwidth excepting the structural design.

Another new stealth technology is plasma stealth technology. Due to the fact that plasma contains an enormous amount of charged particles and free electrons, the plasma will produce a shielding effect when the EM waves hit it. The waves will be absorbed and their reflection direction will be changed simultaneously, thereby realizing stealth effect [18, 19]. Due to engineering limitations, the plasma cannot be too thick, but when the thickness of the plasma is reduced, the attenuation amplitude of the EM waves is reduced too. So how to reduce the plasma thickness while maintaining the stealth effect is a problem that needs to be solved.

Currently, it has become a new research trend to combine plasma with other materials or metasurface to improve stealth effect, which does not need too thick plasma and can achieve RCSR effect well. In 2013, Cross *et al* proposed a plasma-based frequency selective surface (FSS) structure to achieve attenuation of 2–3 dB [20]. In 2017, Ghayekhloo *et al* proposed a checkerboard plasma EM surface, which used a plasma-filled structure as the checkerboard unit to achieve the –10 dB RCSR band including X-band [21]. In 2020, Zhang *et al* proposed a plasma superimposed artificial wave vector metasurface structure to achieve attenuation of 5 dB in X-band [22]. In 2020, Zainud-Deen *et al* proposed a plasma-based frequency selective surface structure, which used a plasma-filled structure as the FSS unit to realize a relatively satisfactory RCSR effect in the X-band, achieving a maximum attenuation of 20 dB [23]. In 2020, Malhat *et al* proposed a plasma-based AMC array, which reported a significant RCSR effect in the 9–13 GHz frequency band [24].

In this paper, based on the above research, we combine plasma with checkerboard metasurface in a different way. We propose a theory and design method of the composite structure of the plasma-based checkerboard metasurface. When we combine metasurface with the plasma, and the attenuation effect of the EM wave is significantly improved. The RCSR frequency bandwidth of the plasma-based checkerboard metasurface is wider than that of the only metasurface and that of the only plasma. Moreover, because of the addition of metasurface, we do not need too thick plasma, which is more convenient for engineering implementation.

2. Checkerboard metasurface establishment and verification

The RCSR of the checkerboard metasurface depends on the backscattering cancellation of the reflected waves, shown when the electromagnetic wave is vertically incident to the metasurface, and the reflected wave will disperse in different directions so as to reduce the RCS in the working band of the metasurface. When designing the unit of the checkerboard metasurface, a layer of metal is coated on the back of the thin dielectric substrate, and a metal patch that can be coupled with the metal back sheet is loaded on the front side to generate magnetic resonance. When the size of the metal patch changes, the phase of the reflected wave changes accordingly. For adjusting the direction

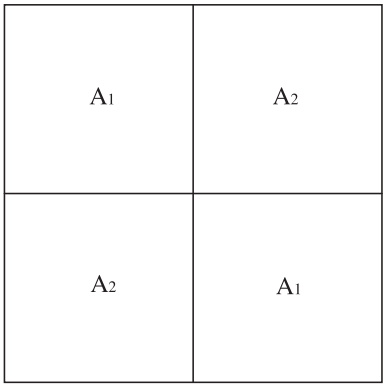


Figure 1. Schematic model used for analyzing the checkerboard metasurface.

of electromagnetic wave reflection, when the reflection phase difference of the two-unit structures satisfies equation (3), a resonant checkerboard metasurface is designed, and in this way the checkerboard metasurface can achieve backscattering cancellation to achieve RCSR. The schematic model used for analyzing the checkerboard structure is shown in figure 1, which is composed of two different AMC units A_1 and A_2 with different reflection phases and the same reflection amplitude when they can achieve total reflection. The reflection phases of unit A_1 and A_2 unit are P_1 and P_2, respectively, and the reflection amplitude of them are respectively E_1 and E_2. The scattering energy of a metal plate with the same size as the metasurface is E_i, and the scattering energy of the metasurface is E_s.

The RCSR of the metasurface and the metal plate can be expressed as equation (1). When the unit A_1 and unit A_2 achieve total reflection, equation (1) can be simplified to equation (2). In order to obtain an RCSR of -10 dB, the relational equation that needs to be satisfied is shown as equation (3), which can be obtained from equation (2). When $P_1-P_2 = 180°$, the RCSR effect of the checkerboard metasurface is best.

$$\begin{aligned}\text{RCS reduction} &= 10\log\left[\frac{\lim\limits_{r\to\infty}\left(4\pi r^2\frac{|E_s^2|}{|E_i^2|}\right)}{\lim\limits_{r\to\infty}[4\pi r^2(1)^2]}\right] \\ &= 10\log\left[\frac{E_1 e^{jp_1}+E_2 e^{jp_2}}{2}\right]^2 \end{aligned} \tag{1}$$

$$\text{RCS reduction} = 10\log\frac{1+\cos(P_1-P_2)}{2} \tag{2}$$

$$143° \leqslant |P_1-P_2| \leqslant 217° \tag{3}$$

Figure 2 depicts the unit structure of the checkerboard metasurface. The dielectric substrate is TLY-5, whose dielectric relative constant is 2.2 and loss tangent is 0.0009, the length of its side is $l = 15$ mm, its thickness is $h = 3.175$ mm, the width of each ring is $w_1 = 0.775$ mm, $w_2 = 1$ mm, $w_3 = 2.1$ mm, and the radius of unit A_1 and unit A_2 are respectively r_1 and r_2. The back side of the substrate is coated with a layer of metal, and the front surface structure is a 'wheel-shaped' metal piece. When the EM wave is incident on the unit's surface, the metal structure on the unit's front side is coupled with the metal plate to generate EM

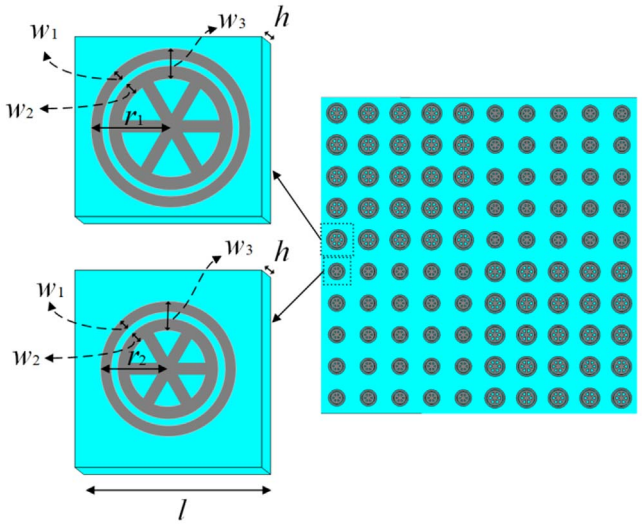


Figure 2. Schematic diagram showing unit structure of the metasurface.

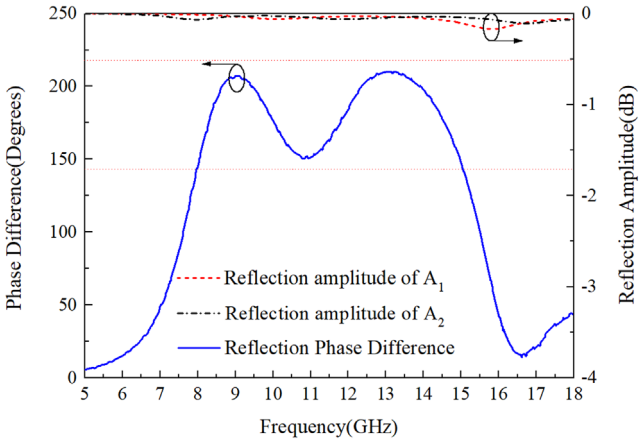


Figure 3. Reflection phase difference and reflection amplitude of A_1 and A_2.

resonance, thereby changing the reflection phase of the EM wave. By fine tuning the size of r, different reflection phases are generated.

The full-wave simulation is performed by the frequency-domain solver of the simulation software Computer Simulation Technology (CST). After parameter sweep and optimization. We select $r_1 = 4.8$ mm, $r_2 = 3.93$ mm. The reflection phase and reflection amplitude of unit A_1 and unit A_2 are shown in figure 3. It is observed that the difference of unit A_1 and unit A_2's reflection phase in the 8–15 GHz band is between 143° and 217°, A_1 and A_2 can both realize total reflection.

The metasurface's overall size is 150 mm × 150 mm and its structure is shown in figure 2. To calculate the RCSR, a metal plate of the same dimensions is used as reference. The EM wave is perpendicularly incident on the metasurface along the z-axis. The total value of monostatic RCSR with the metasurface and the metal plate under different polarized waves is shown in figure 4. The −10 dB RCSR is almost achieved over the frequency band from 8.1 to 14.5 GHz under different polarized waves and the

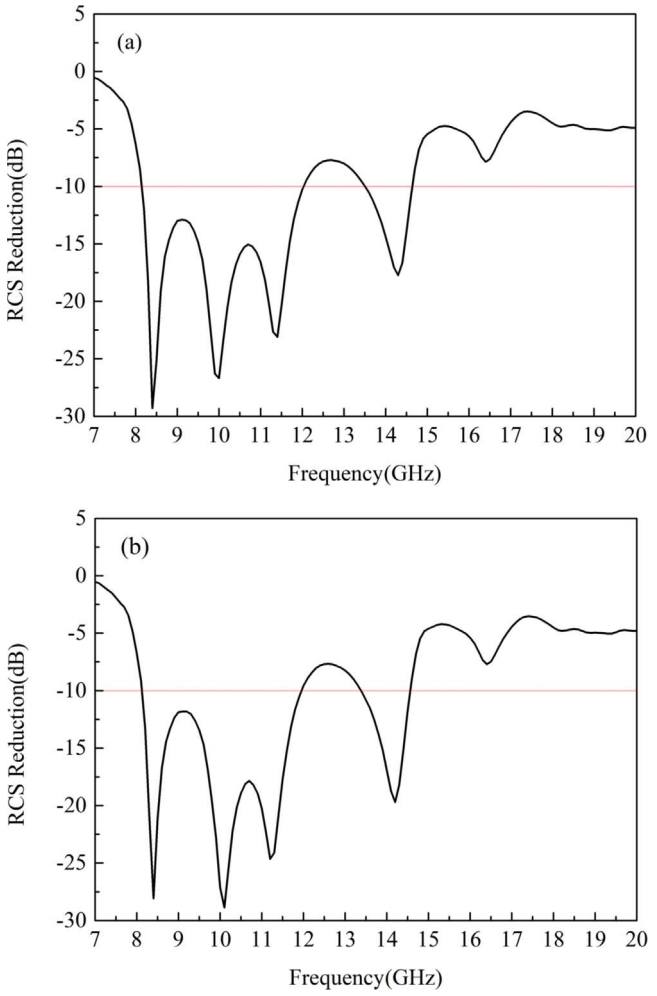


Figure 4. RCSR under (a) x-polarized wave and (b) y-polarized wave.

frequency band is also called the working band of the metasurface. The RCS scatter diagram of the metasurface is shown in figure 5(a). It can be shown that the main lobes of the reflection pattern are distributed in four directions. As a reference, the RCS scatter diagram of a metal plate of the same size as the metasurface is shown in figure 5(b). It can be shown that EM waves are reflected vertically.

3. RCSR by plasma-based checkerboard metasurface

3.1. Analysis of attenuation mechanism of plasma and metasurface with EM waves

Plasma can usually be equivalent to a dielectric, according to the dielectric characteristics of the plasma, its effect on the reflection and absorption of EM waves is primarily affected by its characteristic frequency ω_p and collision frequency ν. This paper presumes that the plasma is uniformly distributed and non-magnetized. The characteristic frequency ω_p of the plasma is determined by the electron density n_e, which is

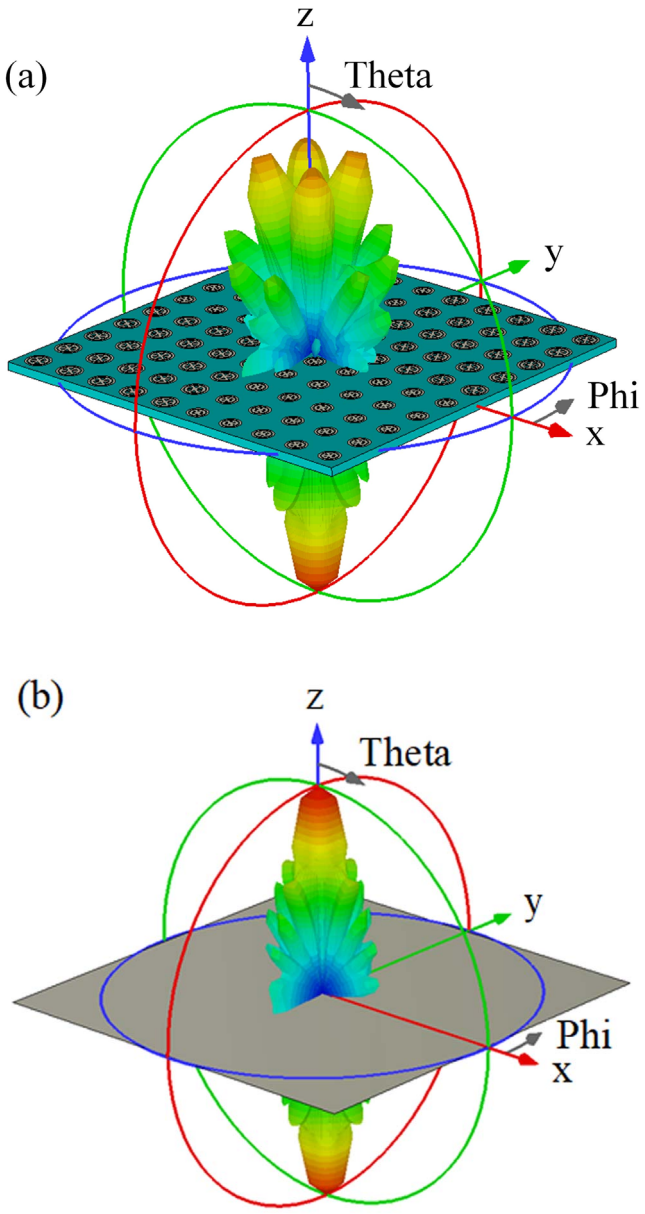


Figure 5. RCS pattern of (a) metasurface and (b) metal plate.

expressed as

$$\omega_{\mathrm{p}} = \sqrt{\frac{n_{\mathrm{e}} e^2}{\varepsilon_0 m_{\mathrm{e}}}} \tag{4}$$

where n_{e} is the electron density per cubic meter, e is the electron charge, m_{e} is the mass of the electron, and $e = 1.6 \times 10^{-19}$ C, $m_{\mathrm{e}} = 9.11 \times 10^{-31}$ kg, $\varepsilon_0 = (1/36\pi) \times 10^{-9}$ F·m^{-1}. The plasma material is introduced with the Drude dielectric model in the simulation software. The model is described in the following:

$$\varepsilon_{\mathrm{r}} = 1 - \frac{\omega_{\mathrm{p}}^2}{\omega^2 + \nu^2} - \mathrm{j}\frac{\nu\omega_{\mathrm{p}}^2}{\omega(\omega^2 + \nu^2)} = \varepsilon' - \mathrm{j}\varepsilon'' \tag{5}$$

$$\sigma = \varepsilon_0 \frac{\nu\omega_{\mathrm{p}}^2}{\omega^2 + \nu^2} = \omega\varepsilon_0\varepsilon'' \tag{6}$$

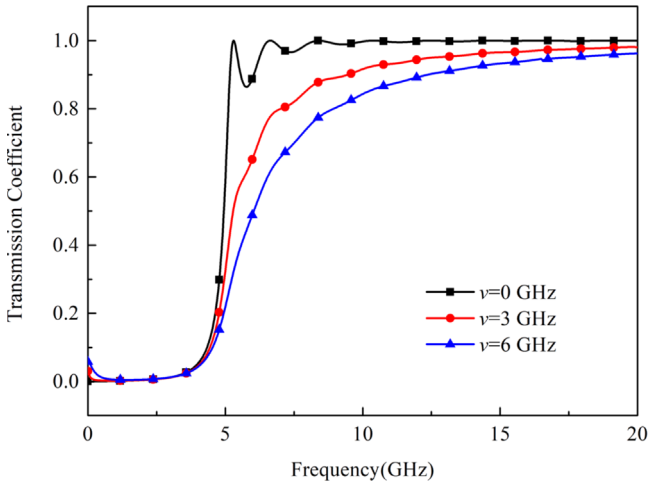


Figure 6. Transmission coefficient of plasma with different collision frequencies.

$$\varepsilon' = 1 - \frac{\omega_{\mathrm{p}}^2}{\omega^2 + \nu^2},\ \varepsilon'' = \frac{\nu\omega_{\mathrm{p}}^2}{\omega(\omega^2 + \nu^2)} \tag{7}$$

where ω, ε_{r}, ε', ε'', σ are, respectively, the frequency of the EM waves, plasma's relative permittivity, the real part of relative permittivity, the imaginary part of relative permittivity, and plasma's electrical conductivity, σ can be expressed as shown in equation (6). When $\nu = 0$ Hz, the plasma is equivalent to a high-pass filter. If $\omega > \omega_{\mathrm{p}}$, the real part of the ε_{r} satisfies $0 < \varepsilon' < 1$, the imaginary part of the ε_{r} satisfies $\varepsilon'' = 0$, the EM waves can enter into the plasma and propagate in it, and the band is called passband; if $\omega < \omega_{\mathrm{p}}$, the real part satisfies $\varepsilon' < 0$, and the imaginary part of the ε_{r} satisfies $\varepsilon'' = 0$, the EM waves cannot enter the plasma and propagate in it, and the band is called cut-off frequency band. The plasma frequency determining the plasma's on and off states is referred to as the cut-off frequency of the plasma. When $\nu \neq 0$ Hz, if $\omega < \omega_{\mathrm{p}}$, the real part of the relative permittivity does not satisfy $\varepsilon' < 0$, so the cut-off frequency does not equal to ω_{p}. The imaginary part of the relative permittivity satisfies $\varepsilon'' > 0$ and becomes smaller as the ω becomes larger so the EM waves will suffer increasing losses as the ω becomes smaller. Therefore, the plasma is no longer equivalent to a high-pass filter.

In order to verify the above theory, CST simulated the transmission coefficient of a plasma whose thickness is $d = 65$ mm, characteristic frequency is $\omega_{\mathrm{p}} = 3 \times 10^{10}$ rad s^{-1}, collision frequency ν is, respectively, 0 GHz, 3 GHz, 6 GHz as shown in figure 6. The EM wave is perpendicularly incident on the plasma along the z-axis direction. It is observed that when ν is 0 Hz, the plasma cut-off frequency is about 4.8 GHz, which is basically equal to its characteristic frequency. When ν is 3 GHz and 6 GHz, the cut-off frequency does not equal to ω_{p}, and there are certain losses in all frequencies, and the transmission coefficient goes down more at lower frequencies. Although if $\nu \neq 0$, the plasma is no longer equivalent to a high-pass filter, it is approximate to a high-pass filter when ν is less than 6 GHz according to figure 6.

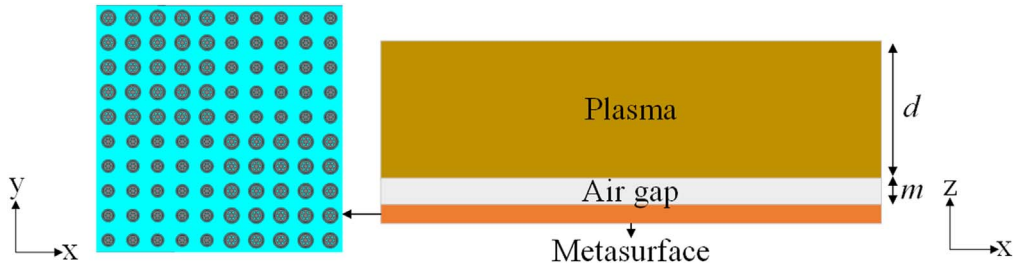


Figure 7. Schematic model of the plasma-based checkerboard metasurface.

The plasma-based checkerboard metasurface is composed of metasurface and plasma. In order to fully exert the plasma-based checkerboard metasurface's low scattering effect on EM waves, it is necessary to enable the metasurface's working frequency higher than the cut-off frequency of the plasma. In this way the plasma can absorb EM waves in the frequency band that are below the plasma's cut-off frequency. In the frequency band that is above the cut-off frequency, most of the EM waves will pass through the plasma and spread out after being reflected by the metasurface, which can reduce the RCS of the plasma-based checkerboard metasurface. When the collision frequency ν of the plasma is 3 GHz, the plasma is approximate to a high-pass filter, in this time the transmission coefficient is over 0.8 in the working band of the metasurface and is low in low frequency band.

3.2. RCSR of plasma-based checkerboard metasurface

We choose the plasma's thickness as $d = 65$ mm which is common in stealth technology. The schematic model of the plasma-based checkerboard metasurface is illustrated in figure 7. The bottom layer is the checkerboard metasurface, and the middle layer is air gap. The upper layer is the plasma layer, the side length of the structure is $L = 150$ mm. The full-wave simulation is performed by CST. In CST, the plasma can be directly described by its own characteristic frequency ω_p and the collision frequency ν.

When the collision frequency ν of the plasma is 3 GHz, the thickness d of the plasma is 65 mm, the thickness m of the air gap is 6 mm, and the characteristic frequency ω_p of the plasma is respectively 1×10^{10} rad s^{-1}, 2×10^{10} rad s^{-1} and 3×10^{10} rad s^{-1}, the RCS is shown in figure 8. It can be observed that the lowest RCS occurs when $\omega_p = 3 \times 10^{10}$ rad s^{-1}.

When the collision frequency ν of the plasma is 3 GHz, the characteristic frequency ω_p of the plasma is 3×10^{10} rad s^{-1}, the thickness d of the plasma is 65 mm, and the thickness of the air gap m is, respectively, 0 mm, 3 mm and 6 mm, the RCS is shown in figure 9. It can be observed that the lowest RCS occurs when $m = 6$ mm.

The RCS of the only plasma and the plasma-based checkerboard metasurface under different polarized waves is shown in figure 10. It can be seen that in the band from 8.1 to 14.5 GHz which is the working band of the metasurface, the RCS of plasma-based checkerboard metasurface is much lower than that of the plasma. Because in the working band of the metasurface, the metasurface can achieve backscattering

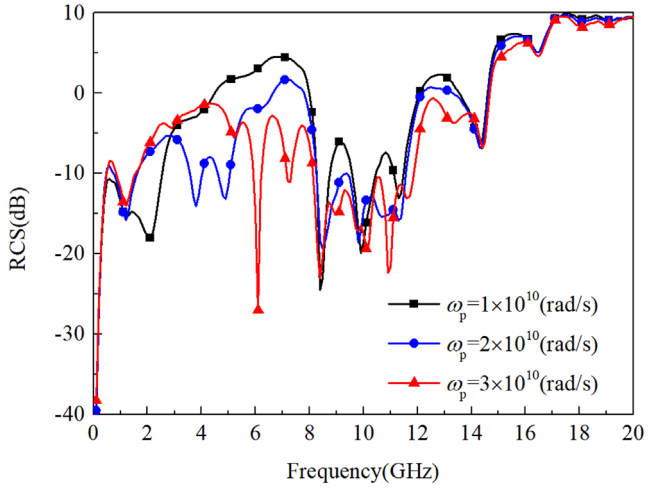


Figure 8. Monostatic station RCS of $\omega_p = 1 \times 10^{10}$ rad s^{-1}, 2×10^{10} rad s^{-1} and 3×10^{10} rad s^{-1}.

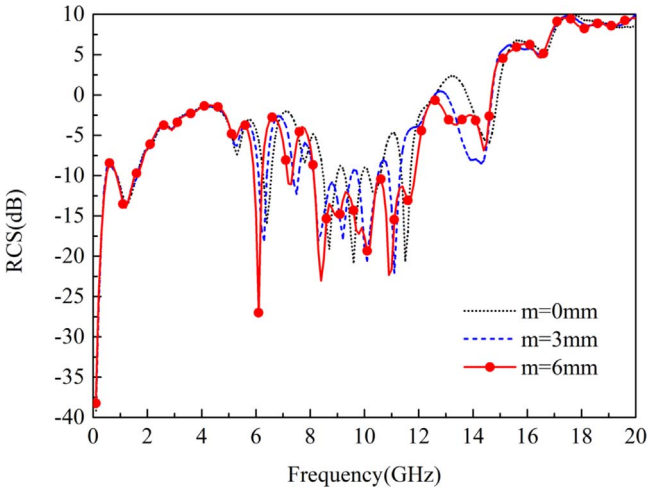


Figure 9. Monostatic RCS of $m = 0$ mm, 3 mm and 6 mm.

cancellation to achieve RCSR. The plasma cannot reduce the RCS in the band because the band is in the passband of the plasma, so the plasma cannot absorb enough EM waves.

The RCS of the only checkerboard metasurface and the plasma-based checkerboard metasurface under different polarized waves is shown in figure 11. It is observed that in the band from 4 to 8.1 GHz, the RCS of plasma-based checkerboard metasurface is much lower than that of the only checkerboard metasurface, because in the band the plasma of the plasma-based checkerboard metasurface plays

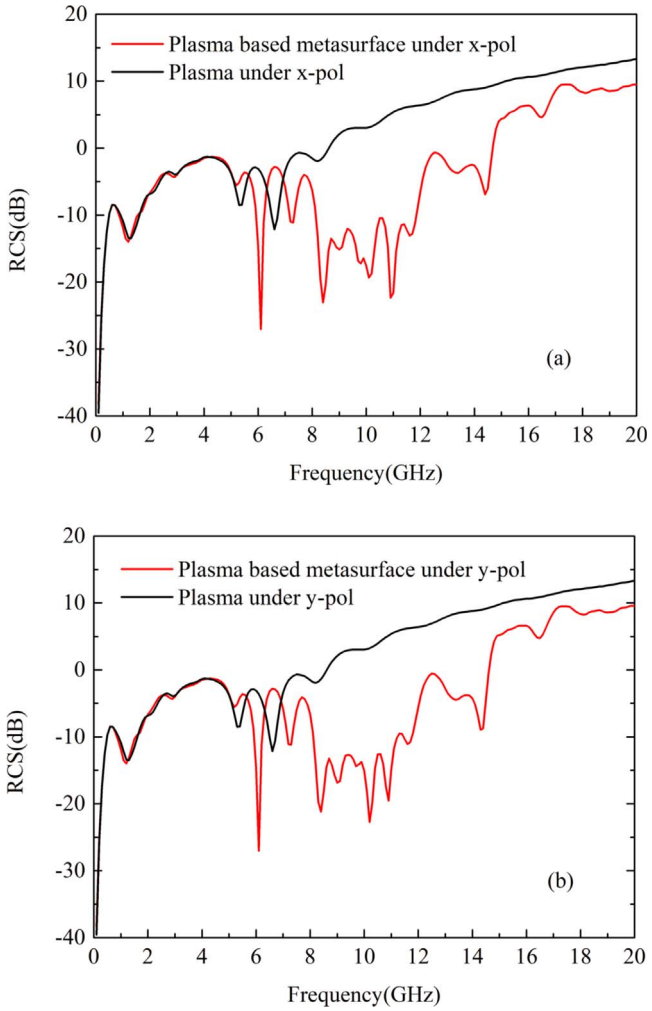


Figure 10. Monostatic RCS of plasma and plasma-based checkerboard metasurface under (a) *x*-polarized wave and (b) *y*-polarized wave.

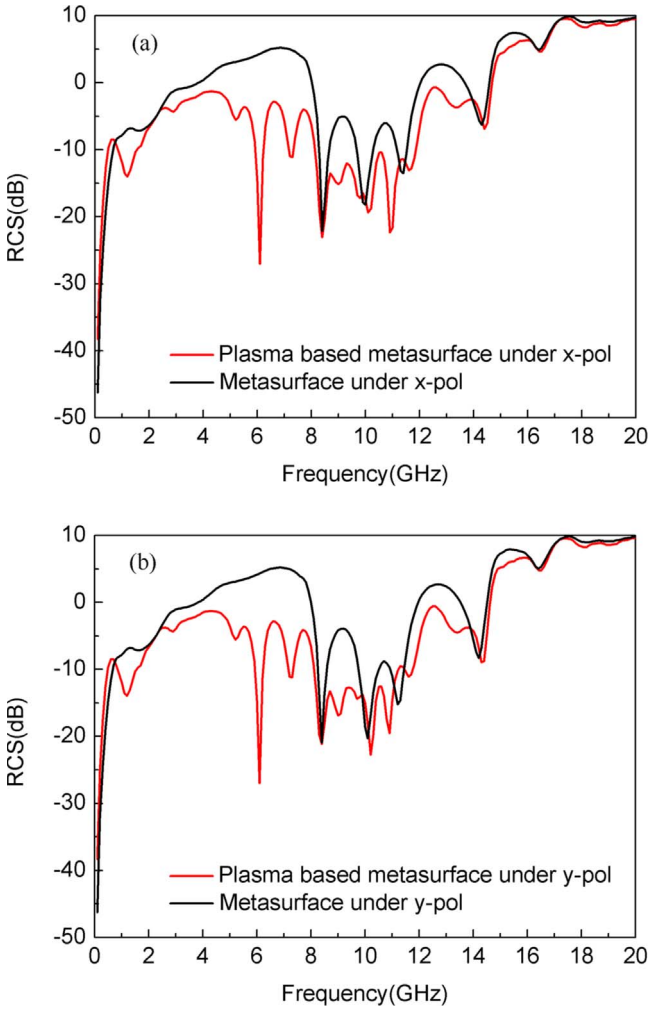


Figure 11. Monostatic RCS of metasurface and plasma-based checkerboard metasurface under (a) *x*-polarized wave and (b) *y*-polarized wave.

a major role in RCSR. As the band is beyond the working frequency band of the metasurface, the metasurface cannot effectively achieve RCS reduction, and the transmission curve of the plasma is shown in figure 6, it is shown that the plasma has a strong absorption of EM waves in the band lower than 8.1 GHz. So, in this band the plasma has a strong absorption of EM waves and plays a major role in RCSR.

In the band from 8.1 to 14.5 GHz, the attenuation effect is enhanced. A very important reason for this is the impedance mismatch at the plasma-air interface which enhances the attenuation effect. When normal incident EM waves are impinging on the plasma-based checkerboard metasurface, the impedance mismatch process generated by plasma-based checkerboard metasurface is shown in figure 12. It is shown in figure 12 that after EM waves are reflected by the metasurface and contact with the plasma, part of the EM waves pass through the plasma, the other part of the EM waves are reflected back to the metasurface due to impedance mismatch at the plasma-air interface, and thus the EM waves will be divided into two parts after they are reflected by the metasurface. The process repeats in this way resulting in a part of the EM waves travelling between the plasma and the metasurface, and each time the angle of reflection is different from the angle of incidence, the angle of scattered waves becomes wider and wider, so the attenuation effect is enhanced.

In the band from 8.1 to 14.5 GHz, another reason to enhance the attenuation effect is the attenuation of plasma to EM waves. Because the plasma we chose in this paper has attenuation effect on EM waves in the band from 8.1 to 14.5 GHz, and the reflection path of EM waves after reflected by the metasurface becomes oblique, the distance in plasma becomes longer, and the attenuation effect of plasma on EM waves is enhanced. Since the plasma-based checkerboard metasurface is spatially symmetric, it imposes almost the same effect on the *y*-polarized wave as on the *x*-polarized wave.

The value of monostatic RCSR of the plasma-based checkerboard metasurface and a metal plate with the same size under different polarized waves is shown in figure 13. The −10 dB RCSR is over the frequency band from 5.8 to 14.7 GHz under different polarized waves which is 2.5 dB wider than that of the only metasurface.

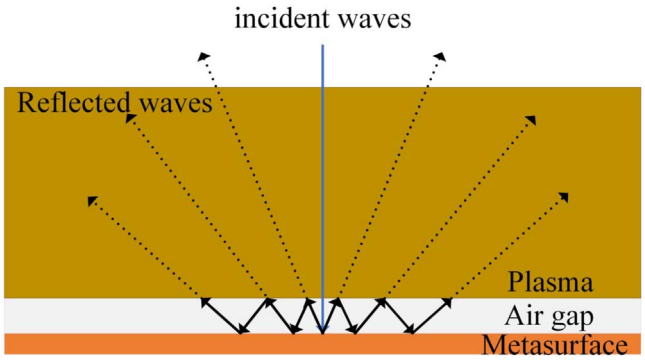


Figure 12. The reflection of EM waves on the plasma-based checkerboard metasurface.

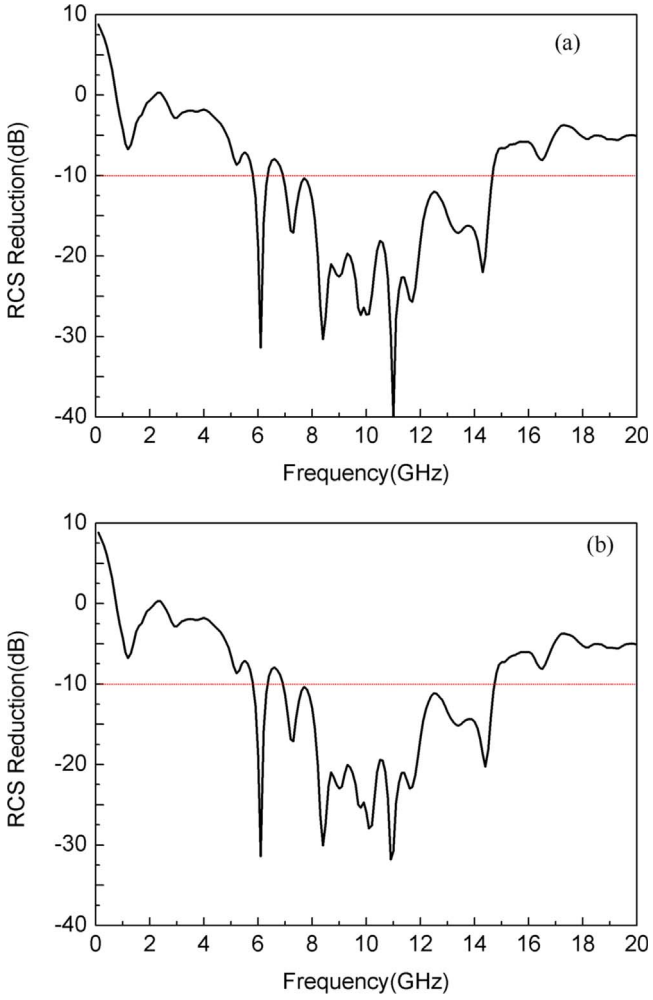


Figure 13. Monostatic RCSR under (a) *x*-polarized wave and (b) *y*-polarized wave.

4. Conclusions

In order to improve RCSR effect, we combine the plasma and the checkerboard metasurface to form a plasma-based checkerboard metasurface. The stealth performance of the proposed structure outperforms either of the only one. The −10 dB RCSR bandwidth of the plasma-based checkerboard metasurface is 2.5 GHz wider than that of the only metasurface. We also analyze the reason of improving the RCSR effect. The rationale of the proposed structure is formulated as follows. In low-frequency band in the non-working area of the metasurface, the plasma plays a key role. Its absorption of EM waves can reduce the RCS of plasma-based checkerboard metasurface. In the working frequency band of the metasurface, the metasurface and the plasma are coupled with each other to reduce the RCS. The metasurface can change the propagation direction of reflected waves so as to reduce the RCS of the plasma-based checkerboard. Because the propagation distance of the reflected waves in the plasma significantly increases, which promotes the absorption of reflected waves by the plasma, the stealth performance of the plasma-based checkerboard metasurface significantly outperforms the only structure, and because of the addition of metasurface, too thick plasma is no longer needed, which is more convenient for engineering implementation.

Despite the above research findings, certain factors that may impose potential effects positively or negatively on plasma-based checkerboard metasurface are not fully considered. For example, consider the conformal problem with aircraft, how to make the plasma-based checkerboard metasurface maintain RCSR performance, and how to make it adjustable in different bands. Our future research interest will be focused in these directions.

References

[1] Yu N F *et al* 2011 *Science* **334** 333
[2] Sun S L *et al* 2012 *Nat. Mater.* **11** 426
[3] Yu N F and Capasso F 2014 *Nat. Mater.* **13** 139
[4] Pendry J B, Schurig D and Smith D R 2006 *Science* **312** 1780
[5] Martin F *et al* 2003 *IEEE Microw. Wireless Compon. Lett.* **13** 511
[6] Smith D R, Pendry J B and Wiltshire M C K 2004 *Science* **305** 788
[7] Su P *et al* 2016 *Sci. Rep.* **6** 20387
[8] Sun H Y *et al* 2017 *Sci. Rep.* **7** 40782
[9] Chen K *et al* 2017 *Opt. Express* **25** 5571
[10] Shelby R A, Smith D R and Schultz S 2001 *Science* **292** 77
[11] Xu H X *et al* 2017 *Ann. Phys.* **529** 1700045
[12] Alrasheed S and Di Fabrizio E 2017 *Appl. Opt.* **56** 3213
[13] Politano A and Chiarello G 2014 *Nanoscale* **6** 10927
[14] Mitrofanov O *et al* 2017 *Sci. Rep.* **7** 44240
[15] Politano A, Viti L and Vitiello M S 2017 *APL Mater.* **5** 035504
[16] Yang Q L *et al* 2014 *Opt. Express* **22** 25931
[17] Galarregui J C I *et al* 2013 *IEEE Trans. Antennas Propag.* **61** 6136
[18] Vidmar R J 1990 *IEEE Trans. Plasma Sci.* **18** 733
[19] Kang W L, Rader M and Alexeff I 1996 *Proc. of 1996 IEEE Int. Conf. on Plasma Science Boston: IEEE* (https://doi.org/10.1109/PLASMA.1996.551505)
[20] Cross L W, Almalkawi M J and Devabhaktuni V K 2013 *IEEE Trans. Plasma Sci.* **41** 948
[21] Ghayekhloo A, Afsahi M and Orouji A A 2017 *IEEE Trans. Plasma Sci.* **45** 603
[22] Zhang W Y *et al* 2020 *J. Phys. D: Appl. Phys.* **53** 065204
[23] Zainud-Deen S H, Malhat H A E A and Shabayek N A 2020 *Plasmonics* **15** 341
[24] Malhat H A, Zainud-Deen S H and Shabayek N A 2020 *Plasmonics* **15** 1025